Published in final edited form as:
J Am Chem Soc. 2009 August 19; 131(32): 11492–11497. doi:10.1021/ja9028928.

Homodimerization and Heterodimerization of Minimal Zinc(II)-Binding Domain Peptides of T-cell Proteins CD4, CD8α, and Lck

Alisa M. Davis[†] and **Jeremy M. Berg**[*]
Contribution from the Laboratory of Molecular Biology, National Institute of Diabetes, Digestive & Kidney Disorders, National Institutes of Health, Bethesda, Maryland 20892

Abstract

Metal-mediated protein oligomerization is an emerging mode of protein-protein interaction. The C-terminal cytosolic domains of T-cell coreceptors CD4 and CD8α form zinc-bridged heterodimers with the N-terminal region of the kinase Lck, with each protein contributing two cysteinate ligands to the complex. Using size exclusion chromatography, ^{1}H NMR, and UV/visible absorption spectroscopy with cobalt(II) as a spectroscopic probe, we demonstrate that small peptides derived from these regions form metal-bridged heterodimers but also homodimers, in contrast to previous reports. The Lck-CD4 and Lck-CD8α cobalt(II)-bridged heterodimer complexes are more stable than the corresponding $(Lck)_2$cobalt(II) complex by factors of 11 ± 4 and 22 ± 9, respectively. These studies were aided by the discovery that cobalt(II) complexes with a cobalt(II)(-Cys-X-X-Cys-)(-Cys-X-Cys-) chromophore show unusual optical spectra with one component of the visible d to d ($^4A_2$ to $^4T_1$(P)) transition red-shifted and well separated from the other components. These results provide insights into the basis of specificity of metal-bridged complex formation and on the potential biological significance of metal-bridged homodimers in T-cells.

Introduction

Specific protein-protein interactions are crucial to many biological processes. Such interactions can be mediated by a variety of structural mechanisms. One such mechanism involves metal ions that bridge between protein partners, with some ligands from each partner coordinated directly to a common metal ion[1–4]. A set of recently characterized examples of such interactions involves complexes between a region from the amino terminus of the T-cell tyrosine kinase Lck and regions from the carboxyl termini of the T-cell surface antigens CD4 and CD8α[5–7]. The structures of heteromeric peptide complexes corresponding to these domains (referred to as “zinc clasp” domains) have been determined in solution by NMR methods[8]. In each of these complexes, two peptides each contribute two cysteinate residues to a common zinc(II) ion. While some additional interactions do occur, the zinc(II)-mediated interactions appear dominant. In their biological context, the formation of these heteromeric complexes is pivotal since the recruitment and activation of Lck to the immunological synapse leads to phosphorylation of CD3 and other proteins on their immunoreceptor tyrosine-based activation motif sequences[9–13]. These phosphorylation events, in turn, trigger recruitment of additional proteins that continue the signal transduction cascade necessary for T-cell activation. These interactions may also be relevant to observations that zinc deficiency leads to impaired immune function including defects in T-cell activation[14–17]. While the basis for these effects have yet to be determined and may be complicated, the Lck-CD4 and Lck-CD8α interactions are potential points where zinc deficiency could have an impact. This notion is supported by

bergj@mail.nih.gov.
[†]Current address: Laboratory of Organic Chemistry, ETH Honggerberg, Zurich, Switzerland

the observation that Lck expression is significantly increased under conditions of zinc deficiency[15, 16].

From a chemical perspective, the observation of specific complexes mediated by peptides that each contribute two cysteinate residues to a common zinc(II) ion raises an important question: To what extent are heteromeric complexes favored over homomeric complexes that could, in principle, have a binding site with the same ligand set? With the Lck-CD4 and Lck-CD8α complexes, this question was partially addressed with the observation that no evidence for the formation of the homomeric Lck-Lck, CD4-CD4, or CD8α -CD8α zinc(II) complexes was observed by NMR under conditions (pH 5.1, 20 mM NaCl, 20 mM sodium acetate) under which the heteromeric Lck-CD4 and Lck-CD8α peptide complexes were stable[8]. This remarkable observation suggests that features present even in these short (19–38 residue) peptides result in substantial preference for the heteromeric over the homomeric complexes, although the extent of this preference could not be deduced from the published data.

The present study was directed toward examining the formation of heterodimeric and homodimeric complexes using a set of peptides derived from these proteins, but limited to the regions surrounding the metal-binding cysteine residues. Specifically, we prepared peptides that were truncated to the metal-binding domain flanked by four to eight residues on each side. These peptides were designed to limit interactions to metal ligation by excluding secondary structural elements that may contribute to dimer stability.

Experimental Section

Size Exclusion Chromatography

All peptides were prepared by solid-phase peptide synthesis and purified by reverse phase high performance liquid chromatography (RP-HPLC) using a C18 semi-preparative column (Vydac, Grace, Deerfield, IL). Peptide samples were prepared under anaerobic conditions. Peptide concentrations were adjusted to 1 to 3 mg/ml. Samples containing zinc contained $ZnCl_2$ (atomic absorption standard, Aldrich, Milwaukee, WI). The pH values of the samples were adjusted to 7.0 with NaOH. Prior to analysis the samples were centrifuged to remove any particulate matter and approximately 100 μL were loaded onto an AKTA FPLC system (GE Healthcare/Amersham Biosciences, Piscataway, NJ) and run over an Amersham Biosciences Superdex Peptide 10/300 GL column. All runs were performed at 0.5 ml/min, 4° C. For samples without metal, the column was prepared by running two column volumes of 10 mM HEPES at pH 7.0, 100 mM NaCl, and 5 mM EDTA buffer to remove any available metal ions. The column was then equilibrated with two column volumes of degassed and filtered running buffer containing 100 mM HEPES at pH 7.0 and 50 mM NaCl that had been incubated with iminodiacetic acid (sodium form) on polystyrene beads. The peptide samples were eluted with 1.5 column volumes of running buffer. For samples containing zinc, the column was equilibrated with 2 column volumes of the filtered metal running buffer containing 100 mM HEPES at pH 7.0, 50 mM NaCl, and 100 μm $ZnCl_2$. Samples with metal were eluted with 1.5 column volumes of this running buffer. Retention times of the species in the samples were measured according to the elution volume of the peak maxima. The column was calibrated with the following molecules and molecular weights: L-tyrosine, 181 Da; oxidized glutathione, 657 Da; synthetic peptide YDLVKHQRTHT, 1,397 Da; synthetic peptide PFRCDHDGGKAFAASHHLKTHVRTCTGE, 3,183 Da; synthetic peptide MVKCFNCGKEGHTARNCRAPRKKGCFNCGKEGHTARNCTER, 4,600 Da.

Nuclear Magnetic Resonance (NMR) Studies

All sample preparation was performed in an anaerobic environment. Samples were prepared by dissolving HPLC-purified, lyophilized peptide in 200 mM deuterated Tris, 50 mM NaCl,

and 10% D_2O to a final concentration for each peptide as follows: Lck, 2 mM; CD4, 1.9 mM; CD8α, 2.1 mM. The samples were initially prepared with a total volume of 1700 to 2300 μL, then aliquoted as 500 to 600 μL samples. Concentrations were confirmed by UV absorption at 278 nm and by detecting sulfhydryl groups with Ellman's reagent. The pH values of the samples were adjusted to between 6.9 and 7.0 with filtered NaOH and HCl. Five hundred to 600 μL of each sample was removed and added to thin-walled, 5 mm O.D. NMR tube (Wilmad-LabGlass, Buena, NJ). $ZnCl_2$ was then added to the remainder of the sample in increments of 0.25 equivalents of peptide concentration. All NMR tubes were sealed with rubber septa.

NMR experiments were carried out at 25° C on a Bruker DMX 600 MHz spectrometer equipped with a triple resonance three-axis pulsed field gradient probe, optimized for ^1H detection. Data were processed using Bruker XWinNMR 2.6 software. The 1-1 echo pulse scheme was used for water suppression[18].

UV/Visible Absorption Spectroscopy with Cobalt(II)

All UV/visible spectra were acquired on a Perkin-Elmer Lambda 25 Spectrophotometer with a 9-cell cuvette changer and Peltier temperature-controlled chamber using Teflon-stoppered, semi-micro, self-masking quartz cuvettes with a path length of 1 cm (Starna Cells. Atascadero, CA). Peptides were prepared from HPLC-purified, lyophilized form and their concentrations determined as described above. All titrations were performed in 200 mM HEPES pH 6.9, 50 mM NaCl buffer that had been degassed and filtered. Metal-binding experiments were carried out by monitoring absorption spectra from 500 to 950 nm. $CoCl_2$ solutions were added and changes in the spectra were recorded until no further significant changes were observed. Starting concentrations for peptides ranged from 50 to 500 μM. Heterodimerization experiments were performed by starting with Lck peptide at concentrations ranging from 50 to 100 μM with 0.5 equivalents of $CoCl_2$ present in the sample. The partner peptides were then titrated into the samples and the changes in the absorption spectra from 500 to 950 nm were monitored.

The data from the heterodimerization experiments were analyzed by principal component analysis as described previously. For each data set, two components could be used to describe all spectra with the coefficients of these components to determine the spectra for the $(Lck)_2Co(II)$ and (Lck)(Peptide)Co(II) species that maximally satisfied the equilibrium constant for the reaction $(Lck)_2Co(II)$ + Peptide⇌(Lck)(Peptide)Co(II) + Lck as a function of added peptide concentration. This analysis results in the estimation of the spectra for pure $(Lck)_2Co(II)$ and (Lck)(Peptide)Co(II) and the equilibrium constants for the reactions.

Results and Discussion

Peptide Sequence Selection

The sequences of the designed peptides, based on the human CD4, CD8α, and Lck sequences are:

CD4, EKKTCQCPHRFQKY (1796 daltons)

CD8α, RRRVCKCPRPVVKSY (1847 daltons)

Lck, ENIDVCENCHYPIVPL (1858 daltons)

with the corresponding molecular weights in parentheses. The CD4 and CD8α peptides include C-terminal tyrosine residues not found in the natural sequences that were added to aid in the determination of peptide concentrations by measurement of the UV absorption due to tyrosine. One additional peptide, a deletion variant of the Lck peptide termed Lck(CEC), with the sequence ENIDVCECHYPIVPL, was also prepared and studied as discussed below.

Formation of Metal-Bridged Homodimers Based on Gel Filtration Chromatography

The first method used to examine the possible formation of zinc-bridged homodimeric complexes was gel filtration chromatography. All three peptides were examined individually on a Superdex peptide column both in the presence and absence of zinc at pH 7. For all three peptides, the addition of excess zinc(II) results in a substantial decrease in retention time consistent with the formation of a complex with an apparent molecular weight approximating that for a species with two peptides and a coordinated zinc ion (Figure 1). This provides initial evidence that these peptides are individually capable of binding zinc and forming homodimeric complexes at neutral pH.

NMR Studies

As an additional probe of homodimeric zinc complex formation, ^{1}H NMR spectroscopy was performed. The resultant spectra are shown in Figure 2. For the CD4 and CD8α peptides, the addition of zinc(II) resulted in some broadening of resonances as well as shifts of resonances associated with histidine HD2 and HE1 protons. However, these changes are modest and no additional well-defined shifted resonances were evident. These results are consistent with the occurrence of zinc binding without the formation of well-defined structures. For the Lck peptide, more substantial changes occurred upon the addition of zinc(II) including the appearance of a number of sharp, shifted resonances. This provides clear evidence for the formation of a homodimeric zinc complex, likely with relatively well-defined three-dimensional structure.

Spectroscopic Studies Using Cobalt(II)

The final method used to examine the formation of homodimeric metal complexes was UV-visible absorption spectroscopy with cobalt(II) as a substitute for zinc[19]. The results of the addition of cobalt(II) to solutions of each of the three peptides are shown in Figure 3. For all three peptides, absorption features in the 550–800 nm region due to d-d transitions provide clear evidence of complex formation. For the CD4 peptide, these features are quite broad and relatively featureless with a maximum extinction coefficient of approximately 250 M^{-1} cm^{-1} (based on the concentration of a presumed Co(II)$(peptide)_2$ complex). This suggests, consistent with the results from the NMR studies, that multiple metal complexes are produced including the tetrahedral complexes with two cysteinate ligands provided by each of two CD4 peptides. These complexes may potentially include the diastereomeric Λ- and Δ- bis-chelates and other species such as five-coordinate complexes or those with histidine ligation (in the case of the CD4 and Lck peptides). For the CD8α peptide, the absorption envelope comprises three major features at approximately 610, 680, and 760 nm. The occurrence and positions of these features are consistent with those anticipated for the three components of a $^{4}A_2$ to $^{4}T_1$(P) transition in a distorted tetrahedral cobalt complex with four cysteinate ligands[20–22]. The relatively low extinction coefficients (<300 M^{-1} cm^{-1} based on the presumed formation of Co(II)$(peptide)_2$ complex) suggests structural inhomogeneity, consistent with the NMR results. For the Lck peptide, an absorption envelope is observed with λ_{max} near 695 nm and shoulders near 660 and 720 nm with a maximum extinction coefficient > 400 M^{-1} cm^{-1}. This is consistent with the formation of a more structurally well-defined tetrahedral Co(II)-tetracysteinate complex. The center of mass of these transitions (plotted as function of energy rather than wavelength) is 14,450 cm^{-1}, similar to values observed for other Co-tetracysteinate complexes[21,22]. Combined with the NMR results, this suggests that metal binding results in the formation of a reasonably well-folded homodimeric complex for the Lck peptide.

The observation of these complexes by absorption spectroscopy allows the thermodynamics of metal binding to be examined by titrating cobalt(II) into solutions of the peptides with the caveat that for the CD4 and CD8α peptides the results will not correspond to parameters for

unique metal complexes. The apparent equilibrium constants for the reactions $(peptide)_2Co(II) \rightleftharpoons 2$ peptide + $Co(II)_{(aq)}$ were determined to be

CD4: $1.5. \pm 0.4 \times 10^{-8}$ M^2

CD8α:° $52 \pm 1 \times 10^{-8}$ M^2

Lck: $8.0 \pm 0.8 \times 10^{-9}$ M^2

These apparent equilibrium constants follow the same trends as that for apparent metal binding-induced folding with the most favorable binding observed for the Lck peptide and the least favorable for the CD4 peptide.

Metal-Bridged Heterodimer Formation

With this demonstration of the formation of homodimeric complexes of these three peptides, we sought to probe the formation of heterodimeric complexes involving the Lck-CD4 and Lck-CD8α pairs. This was accomplished through the titration of either the CD4 peptide or the CD8α peptide into solutions of the preformed $(Lck)_2Co(II)$ complex. The results of these experiments are shown in Figure 4. The addition of the CD4 peptide to the $(Lck)_2Co(II)$ complex results in the conversion of the initial spectrum into a different spectrum with a shoulder near 620 nm, a maximum at 665 nm, and, strikingly, a relatively well separated absorption band with a maximum at 818 nm (Figure 4(A)). Clear isosbestic points are observed at 697 and 764 nm. These results are consistent with the conversion of $(Lck)_2Co(II)$ into the heterodimeric complex (Lck)(CD4)Co(II) upon addition of the CD4 peptide with the (Lck)(CD4)Co(II) complex having one of the three components of the $^4A_2$ to $^4T_1(P)$ transition shifted so that it is separated from the other two components. The center of mass of the transitions (plotted versus energy rather than wavelength) is at 14,900 cm^{-1}, only slightly shifted from that for the $(Lck)_2Co(II)$ complex and within the range observed for other Co-tetracysteinate complexes. The near identity in the average position of these transitions for $(Lck)_2Co(II)$ and (Lck)(CD4)Co(II) is consistent with no difference in coordination number. The isosbestic points indicate that only two species contribute substantially to the spectra and no significant concentration of $(CD4)_2Co(II)$ is produced, consistent with the previously determined equilibrium constants. The larger dispersion in the components of the $^4A_2$ to $^4T_1(P)$ transition for (Lck)(CD4)Co(II) is presumably due to larger distortions from tetrahedral symmetry associated with the (-Cys-X-X-Cys-)(-Cys-X-Cys-)Co(II) complex. Additional studies will be required to elucidate the detailed nature of the distortion responsible for these unusual spectroscopic features.

Similar results were observed for the CD8α peptide (Figure 4(B)). Again, a well-separated red-shifted absorption band is observed with λ_{max} at 817 nm and isosbestic points are present at 690 and 767 nm. These data suggest that $(Lck)_2Co(II)$ can be converted cleanly to (Lck)(CD8α)Co(II) upon the addition of the CD8α peptide.

To test if the spacing between the cysteine residues is, indeed, responsible for the unusual spectral features in the heterodimeric peptide, an additional peptide was synthesized. This peptide, Lck(CEC), has the cysteine residues separated by a single residue due to the deletion of an asparagine residue that is present in the parent Lck peptide. Titration of $(Lck)_2Co(II)$ with Lck(CEC) results in spectral changes similar to those observed with the CD4 and CD8α peptides, as shown in Figure 5. Again, a well-separated component of the $^4A_2$ to $^4T_1(P)$ transition was observed near 820 nm, strongly supporting the notion that this feature is due to the Co(II)(-Cys-X-X-Cys-)(-Cys-X-Cys-) chromophore.

The spectral data from these titrations can be used to determine the equilibrium constants for the ligand exchange reactions $(Lck)_2Co(II)$ + Peptide $\rightleftharpoons$ (Lck)(Peptide)Co(II) + Lck. This was accomplished using principal component analysis to determine component spectra for the

$(Lck)_2Co(II)$ and (Lck)(Peptide)Co(II) complexes subject to the constraint that K = [(Lck)(Peptide)Co(II)][Lck]/[$(Lck)_2Co(II)$][Peptide] is constant over the course of each titration. This analysis resulted in the component spectra shown in Figure 6. The spectra for the $(Lck)_2Co(II)$ complex deduced from the three experiments are nearly identical, supporting the validity of the analysis and the constraints used. The spectra deduced for the (Lck)(Peptide)Co(II) complexes are quite similar to one another. The intensities of the red-shifted component of the $^4A_2$ to $^4T_1(P)$ transition vary with the largest extinction coefficient observed for the CD8α peptide and the smallest for the Lck(CEC) peptide. This appears to be due to the fact that the line width for this transition varies with the narrowest transition observed for the CD8α peptide. Plots of the fractional amount of (Lck)(Peptide)Co(II) in the population as a function of the ratio of the concentration of added peptide to the concentration of Lck peptide are shown in Figure 7. The equilibrium constants deduced from this analysis are 22 ± 9 for the CD8α peptide, 11 ± 4 for the CD4 peptide, and 0.28 ± 0.06 for Lck(CEC). These results demonstrate a substantial preference for heterodimer formation over homodimer formation for the Lck-CD4 and Lck-CD8α pairs. The results with Lck(CEC) reveal that this preference is not an intrinsic property of Co(II)(-Cys-X-X-Cys-)(-Cys-C-Cys-) complexes.

Comparison with Previous Results

We have conclusively shown that the peptides we have studied derived from CD4, CD8α, and Lck do form homodimeric complexes of the form $(peptide)_2M(II)$. This result contrasts with the results of Kim et al.[8]. This may be due to the differences in the peptides studied. In addition, differences in experimental conditions and assay methods may also contribute. In particular, Kim et al. monitored complex formation by NMR at pH 5.1. These low pH conditions were selected for NMR studies to minimize rates of amide hydrogen exchange and were tuned to conditions under which the heterodimeric species were stable. However, given the more than 10-fold differences in stability of the heterodimeric complexes versus the homodimeric complexes, it is likely that the homodimeric complexes were not sufficiently stable to form appreciably under the conditions used. The use of NMR detection also hindered homodimeric complex detection in that the CD4 and CD8α complexes do not show well-dispersed NMR spectra.

Kim et al. also reported isothermal titration calorimetry studies directed toward the determination of the dissociation constants for the Lck-CD4 and Lck-CD8α complexes in the presence of excess zinc[8]. These studies were performed by placing their Lck peptide in the calorimetry cell and titrating in solutions containing their CD4 or CD8α peptides at concentrations of 80 μM with 50 μM zinc. Based on our results, the CD4 and CD8α solutions would contain the homodimeric complexes $(CD4)_2Zn$ and $(CD8\alpha)_2Zn$ complexes at 40 μM concentration with 10 μM excess zinc present. The processes that would occur in the calorimetry cell under these conditions (for the CD4 peptide) are

$$(CD4)_2Zn + Lck \rightleftharpoons (CD4)(Lck)Zn + CD4$$

$$2\ Lck + Zn \rightleftharpoons (lck)_2Zn$$

$$(Lck)_2Zn + CD4 \rightleftharpoons (CD4)(Lck)Zn + Lck$$

Analogous reactions would occur for the CD8α peptide. Given that all of these processes are likely occurring to some extent in the calorimetry cell and that each process has its own enthalpy change, the calorimetry curves presented are difficult to interpret in terms of any particular reaction.

Chemical Implications

One of the initial motivations for this study was the report that the peptides containing -Cys-X-Cys- and -Cys-X-X-Cys- did not homodimerize around bound zinc ions. We have

demonstrated that this observation is due to the choice of conditions and assays used to access complex formation. At neutral pH, we have demonstrated that such homodimerization does occur although these reactions are less favorable than are the heterodimerization reactions.

The heterodimeric Lck-CD4 and Lck-CD8α metal complexes are more stable than the most stable homodimeric complex, $(Lck)_2M(II)$, by more than an order of magnitude. Examination of the amino acid sequences of the peptides used provides one simple potential explanation for this preference. The CD4 and CD8α peptides are both anticipated to be positively charged at neutral pH while the Lck peptide is anticipated to be negatively charged (CD4: 2 K, 1 R, 1 H, 1 E, anticipated charge +3; CD8α: 2K, 4R, anticipated charge +6; Lck: 1H, 1D, 2E, anticipated change −2). The ability of electrostatic interactions to control heterodimer versus homodimer stability has been demonstrated for systems such as the Fos-Jun leucine zipper proteins[23, 24].

Biological Implications

The experiments reported herein are based on peptides that were explicitly chosen to correspond to minimal metal-binding cores of the Lck-CD4 and Lck-CD8α "zinc clasp" complexes. However, these cores are parts of larger domains that are, in turn, components of larger proteins. Most importantly, these domains are very closely juxtaposed to the plasma membrane as CD4 and CD8α are type I membrane proteins while Lck is linked to the membrane via both N-terminal myristoylation and palmitoylation on Cys-3[25, 26]. The close proximity of the metal-binding domains with the plasma membrane could substantially affect the accessible conformations and local concentrations of the metal-binding regions. Thus, detailed comparison of the metal affinities determined for these peptides with the affinities of other proteins is not justified. One observation relevant to future studies of this point is that Lck associates with more with CD4 than with CD8 in immature $CD4^+CD8^+$ T-cells[27].

The discovery that these sequences can, in fact, form metal-bridged homodimeric species has several implications. First, the association of CD4 and CD8α with Lck through a bridging zinc ion had been envisaged as a reaction between metal-free peptides and zinc to form a zinc clasp-based complex. However, it appears likely that CD4, Lck, and, particularly, CD8α may form metal-bridged homodimers prior to association. This is particularly true since CD8α can form CD8α-CD8α dimers stabilized by a range of interactions[28, 29]. This might place the C-terminal tails from the components of such a dimer in suitable proximity for complex formation.

Second, the occurrence of Lck homodimers may explain the observation that increased phosphorylation and activation of Lck occurs in the presence of micromolar concentrations of Zn(II) in murine lymphoma cells overexpressing Lck[30]. The authors attribute this effect to replacement of Mg(II) by Zn(II) as the stabilizing divalent metal ion for ATP in the kinase domain. An alternative hypothesis is that zinc promotes homodimerization and cross-phosphorylation with the Lck dimer.

Summary

We have shown that minimal metal-binding peptides derived from the T-cell proteins CD4, CD8α and Lck are able to form metal-bridged homodimeric complexes, in contrast to previous reports. Further, examination of the related heterodimeric complexes via UV/visible absorption spectroscopy using cobalt(II) as a spectroscopic probe revealed an unusual feature in the spectral envelope, namely a component of the $^4A_2$ to $^4T_1(P)$ d-d transition that is shifted to 820 nm in the Co(II)(-Cys-X-X-Cys-)(-Cys-X-Cys-) complexes. This is consistent with the fact that subtle differences in cobalt(II) coordination geometry can result in significant changes in the splitting of this transition. Furthermore, these results may have implications for interpreting the effects of zinc ions on T-cell signal transduction processes.

Acknowledgments

This work was supported by the NIH Intramural Program through the National Institute of Diabetes and Diabetes and Kidney Diseases and the National Institute of General Medical Sciences. This was completed as part of the Graduate Partnership Program with the Johns Hopkins University Program in Molecular Biophysics. We thank Christopher Jaroniec, Jinfa Ying, Beat Vogeli and Ananya Majumdar for assistance with acquiring NMR spectra, and Drs. Peter Kim and Barbara Amman for useful discussions.

References

1. Baker EN, Blundell TL, Cutfield JF, Cutfield SM, Dodson EJ, Dodson GG, Hodgkin DM, Hubbard RE, Isaacs NW, Reynolds CD, et al. The structure of 2Zn pig insulin crystals at 1.5 A resolution. Philos Trans R Soc Lond B Biol Sci 1988;319:369–456. [PubMed: 2905485]
2. Cunningham BC, Bass S, Fuh G, Wells JA. Zinc mediation of the binding of human growth hormone to the human prolactin receptor. Science 1990;250:1709–1712. [PubMed: 2270485]
3. Bixby KA, Nanao MH, Shen NV, Kreusch A, Bellamy H, Pfaffinger PJ, Choe S. Zn $^{2+}$-binding and molecular determinants of tetramerization in voltage-gated K^+ channels. Nat Struct Biol 1999;6:38–43. [PubMed: 9886290]
4. Hopfner KP, Craig L, Moncalian G, Zinkel RA, Usui T, Owen BA, Karcher A, Henderson B, Bodmer JL, McMurray CT, Carney JP, Petrini JH, Tainer JA. The Rad50 zinc-hook is a structure joining Mre11 complexes in DNA recombination and repair. Nature 2002;418:562–566. [PubMed: 12152085]
5. Hoeveler A, Malissen B. The cysteine residues in the cytoplasmic tail of CD8 alpha are required for its coreceptor function. Mol Immunol 1993;30:755–764. [PubMed: 8099195]
6. Huse M, Eck MJ, Harrison SC. A Zn $^{2+}$ ion links the cytoplasmic tail of CD4 and the N-terminal region of Lck. J Biol Chem 1998;273:18729–18733. [PubMed: 9668045]
7. Lin RS, Rodriguez C, Veillette A, Lodish HF. Zinc is essential for binding of p56(lck) to CD4 and CD8alpha. J Biol Chem 1998;273:32878–32882. [PubMed: 9830036]
8. Kim PW, Sun ZY, Blacklow SC, Wagner G, Eck MJ. A zinc clasp structure tethers Lck to T cell coreceptors CD4 and CD8. Science 2003;301:1725–1728. [PubMed: 14500983]
9. Ehrlich LI, Ebert PJ, Krummel MF, Weiss A, Davis MM. Dynamics of p56lck translocation to the T cell immunological synapse following agonist and antagonist stimulation. Immunity 2002;17:809–822. [PubMed: 12479826]
10. Li QJ, Dinner AR, Qi S, Irvine DJ, Huppa JB, Davis MM, Chakraborty AK. CD4 enhances T cell sensitivity to antigen by coordinating Lck accumulation at the immunological synapse. Nat Immunol 2004;5:791–799. [PubMed: 15247914]
11. Palacios EH, Weiss A. Function of the Src-family kinases, Lck and Fyn, in T-cell development and activation. Oncogene 2004;23:7990–8000. [PubMed: 15489916]
12. Van Laethem F, Sarafova SD, Park JH, Tai X, Pobezinsky L, Guinter TI, Adoro S, Adams A, Sharrow SO, Feigenbaum L, Singer A. Deletion of CD4 and CD8 coreceptors permits generation of αβT cells that recognize antigens independently of the MHC. Immunity 2007;27:735–750. [PubMed: 18023370]
13. Kappes DJ. CD4 and CD8: hogging all the Lck. Immunity 2007;27:691–693. [PubMed: 18031691]
14. Beck FW, Prasad AS, Kaplan J, Fitzgerald JT, Brewer GJ. Changes in cytokine production and T cell subpopulations in experimentally induced zinc-deficient humans. Am J Physiol 1997;272:E1002–E1007. [PubMed: 9227444]
15. Taylor CG, Giesbrecht JA. Dietary zinc deficiency and expression of T lymphocyte signal transduction proteins. Can J Physiol Pharmacol 2000;78:823–828. [PubMed: 11077983]
16. Moore JB, Blanchard RK, McCormack WT, Cousins RJ. cDNA array analysis identifies thymic lck as upregulated in moderate murine zinc deficiency before T-lymphocyte population changes. J Nutr 2001;131:3189–3196. [PubMed: 11739864]
17. Hosea HJ, Rector ES, Taylor CG. Zinc-deficient rats have fewer recent thymic emigrant (CD90+) T lymphocytes in spleen and blood. J Nutr 2003;133:4239–4242. [PubMed: 14652378]
18. Sklenar V, Bax A. Spin-echo water suppression for the generation of pure-phase two-dimensional NMR spectra. Journal of Magnetic Resonance 1987;74:469–479.

19. Maret W, Vallee BL. Cobalt as probe and label of proteins. Methods Enzymol 1993;226:52–71. [PubMed: 8277880]

20. Figgis, BN. Introduction to Ligand Fields. New York: Interscience; 1966.

21. Lane RW, Ibers JA, Frankel RB, Paperfthymiou GC, Holm RH. Synthetic Analogues of the Active Sites of Iron-Sulfur Proteins. 14. Synthesis, Properties, and Structures of Bis(o-xylyl-α-α'-dithiolato) ferrate(II,III) Anions, Analogues of Oxidized and Reduced Rubredoxin Sites. Journal of the American Chemical Society 1977;99:84–98. [PubMed: 830690]

22. Krizek BA, Merkle DL, Berg JM. Ligand variation and metal ion binding specificity in zinc finger peptides. Inorganic Chemistry 1993;32:937–940.

23. O'Shea EK, Rutkowski R, Stafford WF 3rd, Kim PS. Preferential heterodimer formation by isolated leucine zippers from fos and jun. Science 1989;245:646–648. [PubMed: 2503872]

24. O'Shea EK, Rutkowski R, Kim PS. Mechanism of specificity in the Fos-Jun oncoprotein heterodimer. Cell 1992;68:699–708. [PubMed: 1739975]

25. Johnson DR, Bhatnagar RS, Knoll LJ, Gordon JI. Genetic and biochemical studies of protein N-myristoylation. Annu Rev Biochem 1994;63:869–914. [PubMed: 7979256]

26. Paige LA, Nadler MJ, Harrison ML, Cassady JM, Geahlen RL. Reversible palmitoylation of the protein-tyrosine kinase p56lck. J Biol Chem 1993;268:8669–8674. [PubMed: 8473310]

27. Wiest DL, Yuan L, Jefferson J, Benveniste P, Tsokos M, Klausner RD, Glimcher LH, Samelson LE, Singer A. Regulation of T cell receptor expression in immature CD4+CD8+ thymocytes by p56lck tyrosine kinase: basis for differential signaling by CD4 and CD8 in immature thymocytes expressing both coreceptor molecules. J Exp Med 1993;178:1701–1712. [PubMed: 8228817]

28. Chang HC, Tan K, Ouyang J, Parisini E, Liu JH, Le Y, Wang X, Reinherz EL, Wang JH. Structural and mutational analyses of a CD8αβ heterodimer and comparison with the CD8αα homodimer. Immunity 2005;23:661–671. [PubMed: 16356863]

29. Shore DA, Teyton L, Dwek RA, Rudd PM, Wilson IA. Crystal structure of the TCR co-receptor CD8αα in complex with monoclonal antibody YTS 105.18 Fab fragment at 2.88 A resolution. J Mol Biol 2006;358:347–354. [PubMed: 16530222]

30. Pernelle JJ, Creuzet C, Loeb J, Gacon G. Phosphorylation of the lymphoid cell kinase p56lck is stimulated by micromolar concentrations of Zn^{2+} FEBS Lett 1991;281:278–282. [PubMed: 2015905]

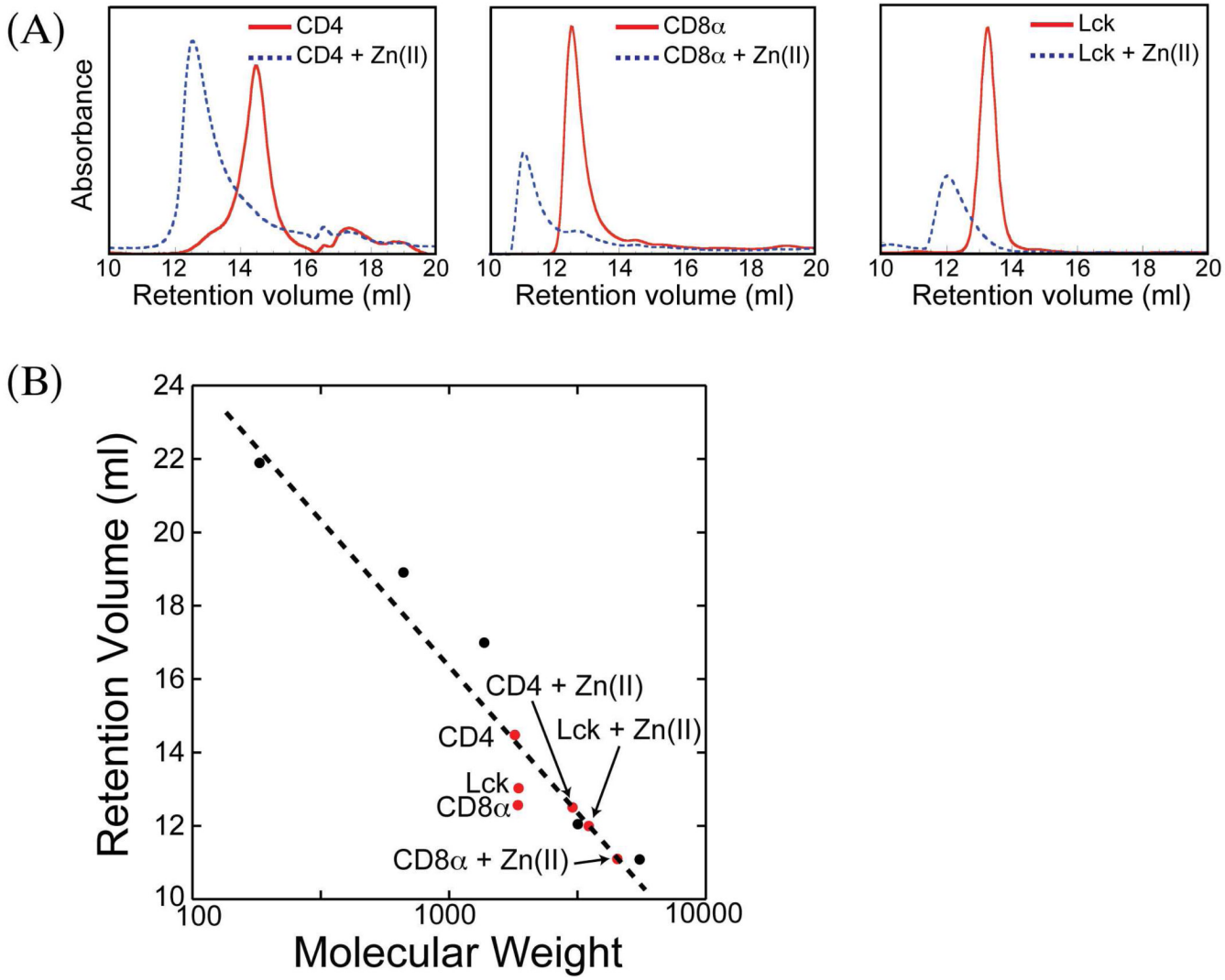

Figure 1.

Size exclusion chromatography of Lck, CD4, and CD8α peptides with and without Zn(II). (A) Individual chromatograms and retention volumes for each peptide with and without Zn(II). (B) Calibration curve for Superdex Peptide column. Molecular weight standards are points in black, experimental points are in red.

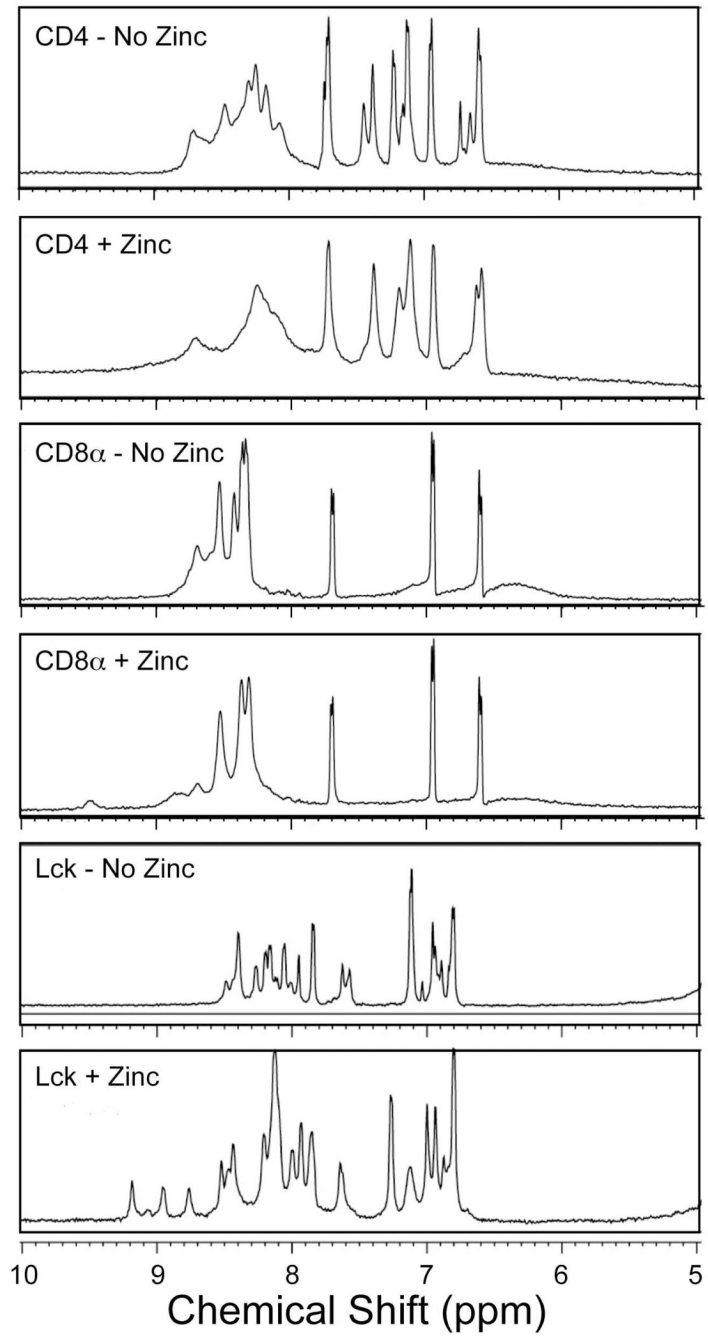

Figure 2.

^{1}H NMR spectra of peptides with and without Zn(II) in H_2O. The aromatic and amide proton regions are shown. Samples were prepared as described in the Experimental Section.

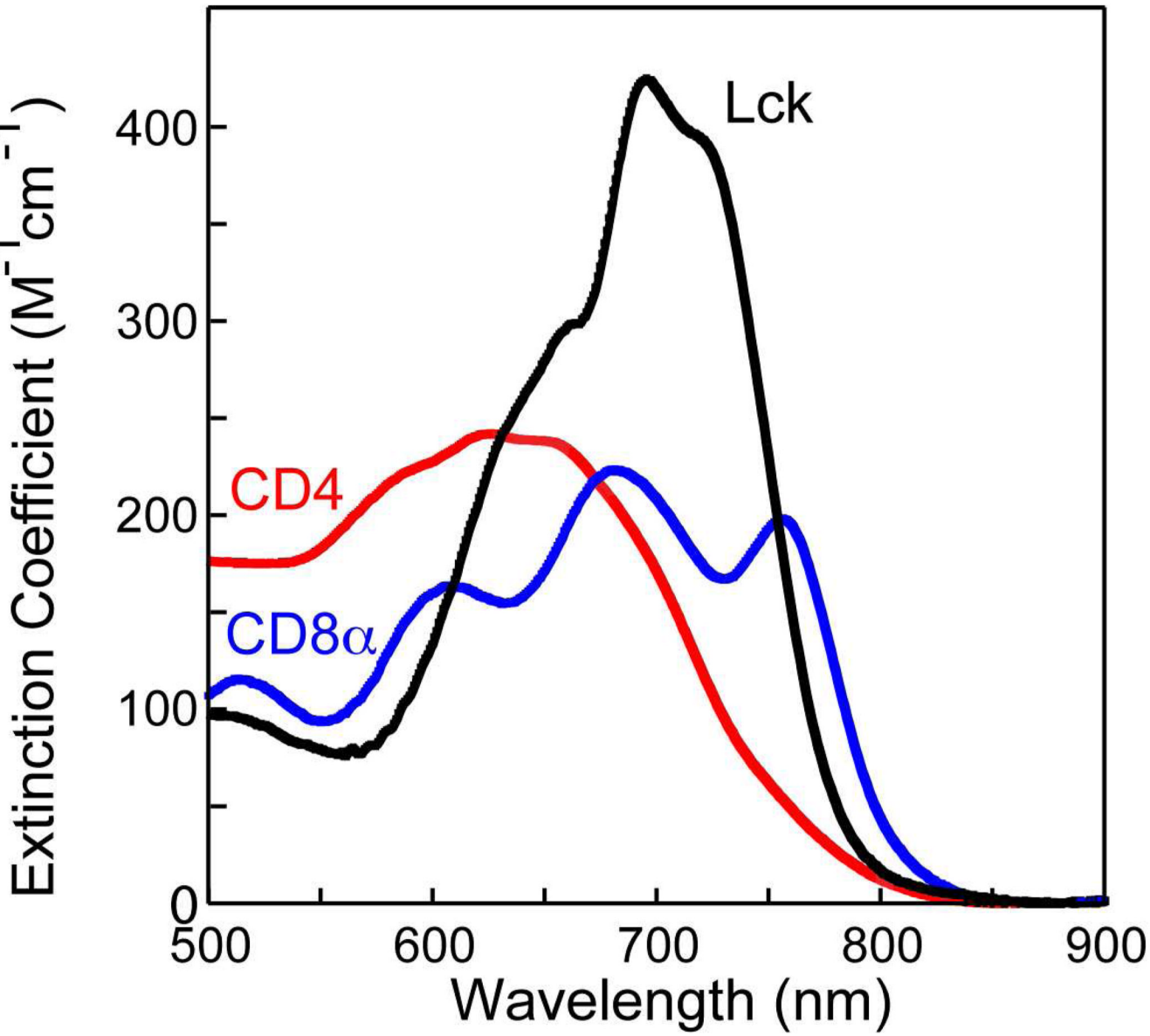

Figure 3.
Absorption spectra of homodimeric (Peptide)Co(II) complexes in the visible region. Estimated molar extinction coefficients are shown based on the presumed concentration of the complexes.

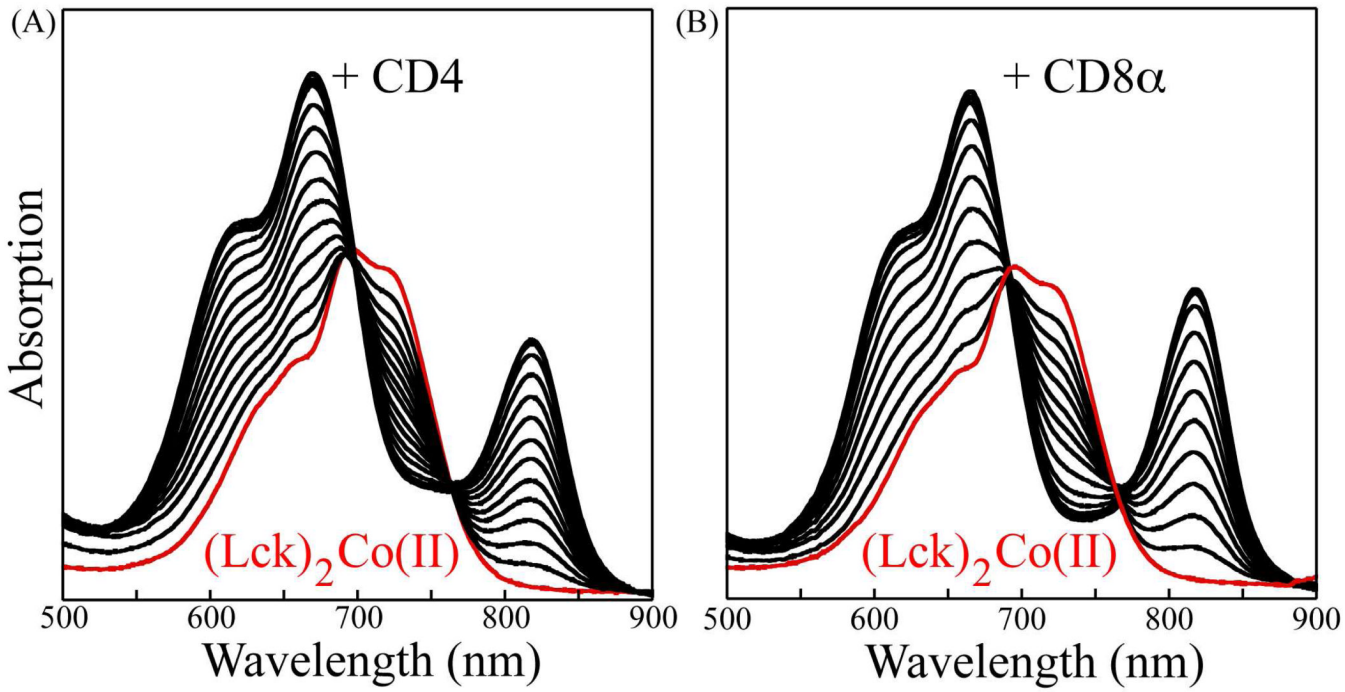

Figure 4.
Absorption spectra of competitive titration of $(Lck)_2Co(II)$ complex with CD4 (A) and CD8α (B). The initial spectra due to $(Lck)_2Co(II)$ are shown in red.

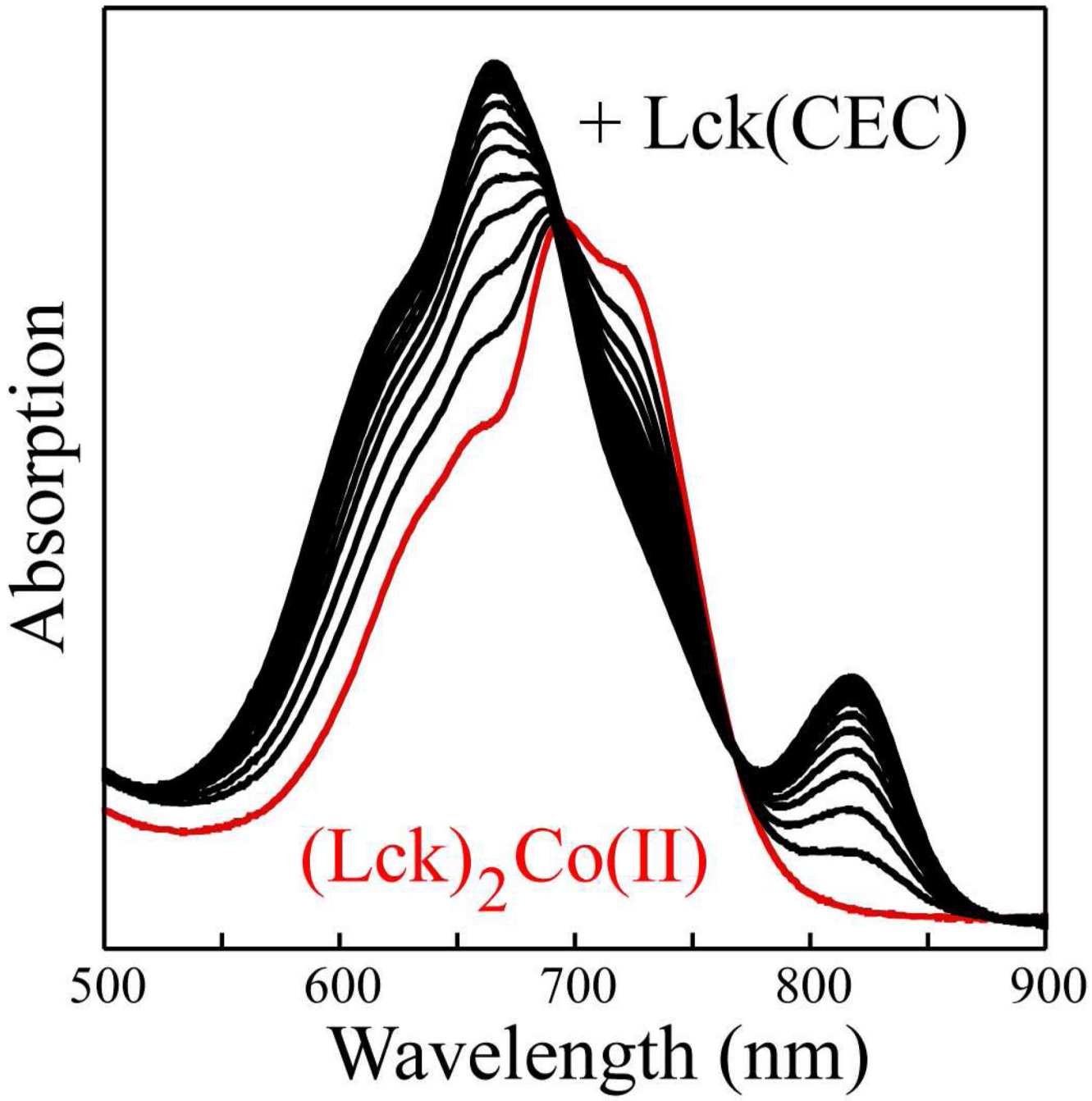

Figure 5.
Absorption spectra of competitive titration of $(Lck)_2Co(II)$ complex with Lck(CEC) peptide. The initial spectrum due to $(Lck)_2Co(II)$ is shown in red.

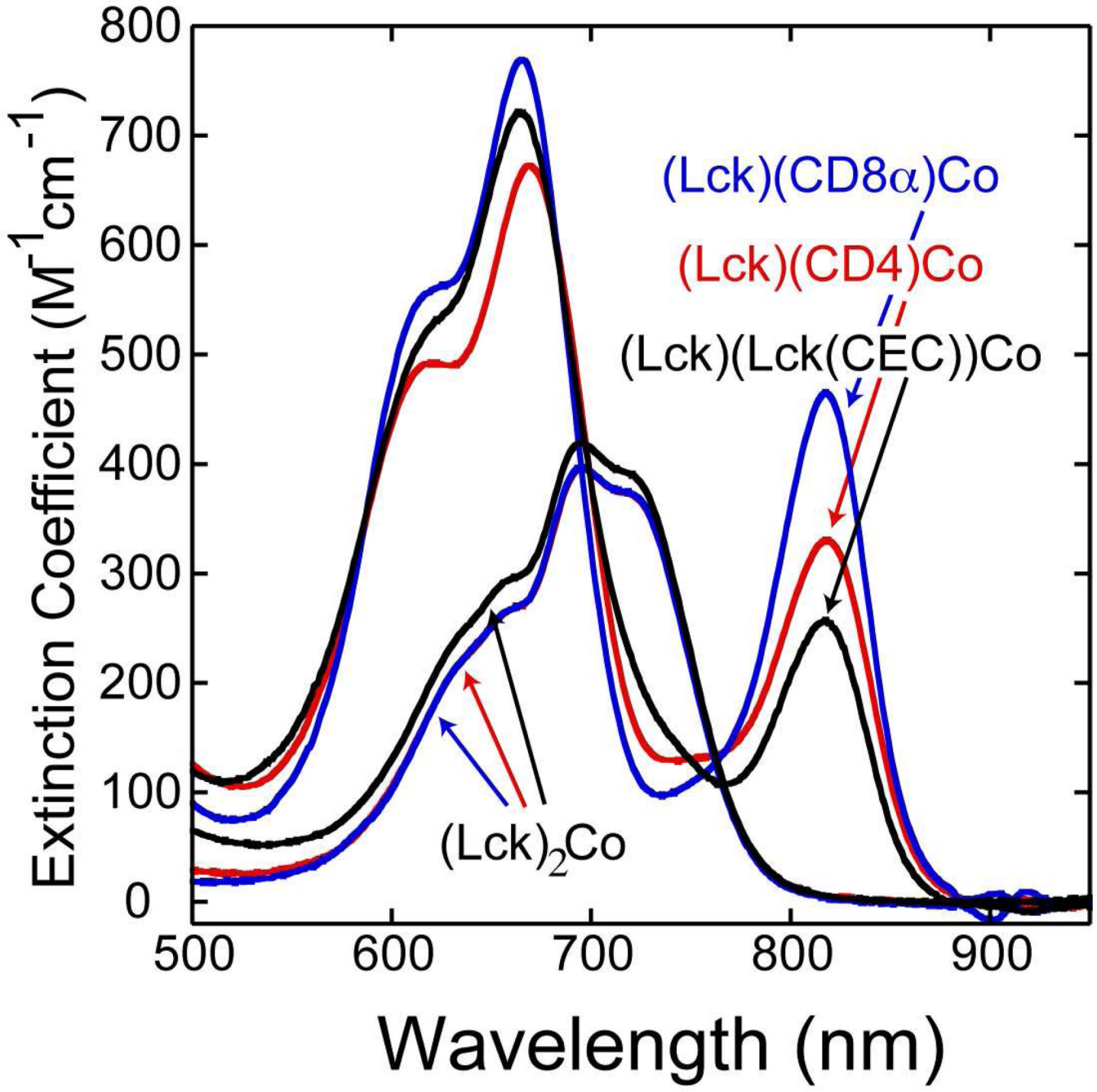

Figure 6.
Component spectra deduced for (Lck)(CD4)Co(II) (red), for (Lck)(CD8α)Co(II) (blue), and for (Lck)(Lck(CEC))Co(II) (black) as well as deduced spectra for $(Lck)_2Co(II)$ from the three competitive titrations.

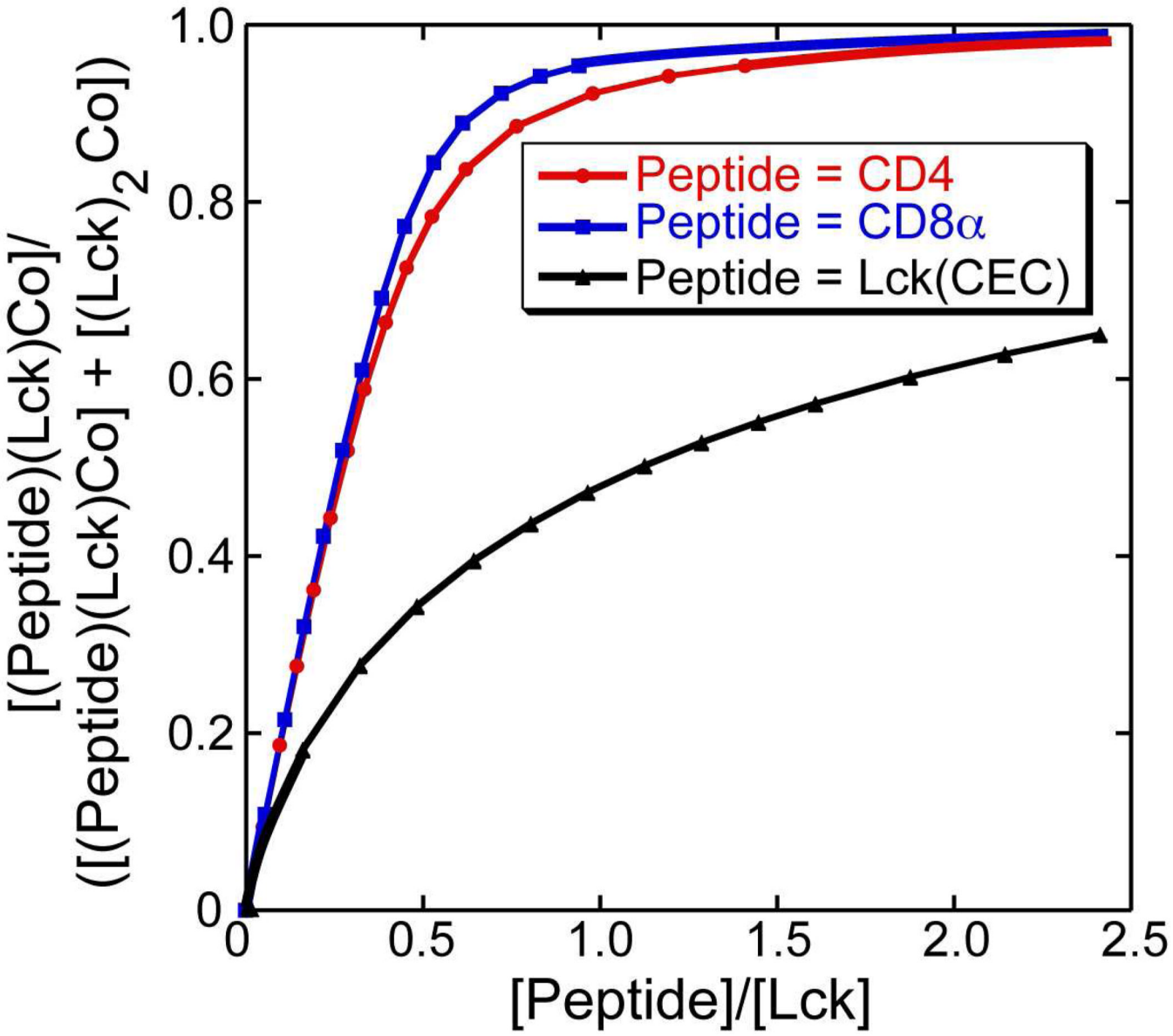

Figure 7.
Fractions of the heterodimeric complexes plotted as a function of CD4, CD8α, or Lck(CEC) concentration relative to Lck concentration over the course of competitive titrations.